University of Thi-Qar Journal Vol. 13 No.4 DEC 2018
Web Site: **https://jutq.utq.edu.iq/index.php/main**
Email: journal@jutq.utq.edu.iq

Study of Dielectric properties for porous silicon prepared by Anodization

Salah M. Abd Ulaziz **S.mehdi@uos.edu.iq**
University of Sumer/Natural Sciences Department
Thi-Qar / Iraq

Abstract

The nanostructure for porous silicon (PS) films is produced by anodization of p-type silicon chip with current consistency (15 mA/cm^2), etching time about 10 min and HF concentration (32%) to the formation nanosized pore order with a dimension of around few hundreds nanometric. The films were featured by the measurement of atomic force microscopy (AFM) in the Baghdad university, X-Ray diffraction (XRD) and FTIR spectroscopy characteristics in the technological university. I am having appraising crystallites size from XRD about nanoscale for porous silicon and AFM proves the nanometric size.

Chemical fictionalizations through the electrochemical etching clear on superficies chemical structure of PS. The etching possess disproportionate microstructures that include Si-H clusters in (Si_3-SiH), sparse in amorphous silica matrix and Si-H_2 scissor mode. From the FTIR testing appeared that the Si suspending bonds of the as- produced PS layer have massive quantities of Hydrogen to form weak Si–H bonds related to Si–H stretch (Si_3-SiH) and Si-H stretch (Si_2-SiH).

The AC electrical properties were measured with LCR meter analyzer the frequency between 50 Hz and 5 MHz. for capacitance, dielectric and loss tangent (tan δ_D) to balk silicon and porous silicon have been done in the ministry of science and technology.

Keywords: Dielectric**;** capacitance; dielectric; loss tangent.

University of Thi-Qar Journal Vol. 13 No.4 DEC 2018
Web Site: **https://jutq.utq.edu.iq/index.php/main**
Email: journal@jutq.utq.edu.iq

دراسة الخواص العزلية للسيلكون المسامي المحضر بالانوذة

الخلاصة

تم تحضير أغشية السليكون المسامي النانوية بطريقة التنميش الكهروكيميائي لرقائق السليكون من النوع القابل مع كثافة تيار (15 ملي امبير/سم ^{2}) وزمن تنميش (10 دقائق) وحامض هايدروفلوريك بتركيز (32%) لتكوين حفر بأحجام نانوية منظمة بحدود مئات قليلة من الأبعاد النانومترية وتم تشخيص الأغشية من قياسات حيود الأشعة السينية ومطيافية تحويلات فورير للأشعة تحت الحمراء في الجامعة التكنولوجية وخواص مجهر القوى الذري في جامعة بغداد . من حيود الأشعة السينية تم تخمين الحجم البلوري للسليكون المسامي بالمقياس النانو ومجهر القوى الذري يؤكد على ان الحجم بالنانومتر.

كما تم تحديد المجاميع الفعالة الكيميائية خلال التنميش الكهرو كيمياوي تظهر على سطح المركب الكيميائي للسليكون المسامي .عملية التنميش الكهروكيميائي التي تحوي على تراكيب مايكرويه غير متجانسة التي تحوي (Si-H) في عناقيد (Si_3-SiH) المشتتة في السليكا العشوائية و نمط ($Si-H_2$). من تحليلات تحويلات فورير للاشعة تحت الحمراء أظهرت أواصر السليكون المتدلية لطبقة السليكون المسامي كما تم ترسيبها حيث تحوي كمية كبيرة من الهيدروجين على شكل أواصر Si–H الضعيفه تتعلق ب (Si–H) تمتد (Si_3-SiH) و (Si_2-SiH) .

تم قياس الخواص الكهربائية للتيار المتناوب AC مع جهاز(LCR) في وزارة العلوم والتكنولوجيا ضمن تردد بين (50 Hz and 5 MHz) للسعة و ثابت العزل الكهربائي وعامل الفقد للسليكون و السليكون المسامي.

1. INTRODUCTION

Porous silicon (PS) can be considered as a silicon crystal having a network of voids in it. The nanosized voids in the Si bulk result in a sponge-like structure of pores and channels surrounded with a skeleton of crystalline Si nanowires [1]. Porous silicon (PS) is prepared by electrochemical etching of silicon samples. Silicon was composed crystallites by this means can existing diameters changing from collectives of nanometers to tens of micrometers , counting on brewing parameters (sample type, current density, anodization time, and current density) . This feature, that is, the prospect of porosity hegemony, creates PS apropos for several applications on gas sensing [2], solar cells [3], and Porous silicon nanowires for lithium rechargeable batteries [4].

The substance characteristic of PSi for its utilize as a low-loss RF sample were checked by a little collections. Moreover specifically, description of the dielectric characteristics of PSi has been notify for frequencies extend from direct current (DC) up to frequencies of a few hundreds of megahertz employ capacitor and inductor building integrated on PSi strata's [5]. Porous silicon because of its peerless charcteristic of spatial confinement, dimensionality (large active) and decrease of reflection losses, etc. stimulated many applications in different fields: light emitting diodes[6], optical sensors[7], interference filters[8], wave guides[9], and biomedical applications [10].

Several research collection have utilized porous silicon (PS) strata's as an antireflection coating to reduce the surface reflectance[11]. Decreasing the front surface reflectance of crystalline silicon (Si) solar cells is one of the most important issues for improving the cells efficiency[12]. The refractive index for PS strata's relies on its porosity and its morphology, and the optimization of these laborers may work to an ideal antireflection coating for silicon solar cells [13].

2. Experimental

The sample utilized in this search is p-type (100) Si chip with resistivity (1.4-5) Ω.cm ply 508±15 μm. The back faces of chips were implanted with boron put up with by Aluminum metallization to get better the regular of current flux during electrochemical etching and to procure symmetrical porous stratums [14].

The porous silicon substrate was primed by electrochemical etching method in a solution of 32% hydrofluoric acid and 99.9% ethanol at etching time was 10 min, and the current density was 15 mA/cm^2, after anodization, the samples were washed-up in pentane and ethanol and dried in nitrogen (N_2). Ethanol is collected to the hydrofluoric acid to deflate its surface tension that way letting the H_2 gas composed through the reaction beating off, banning it from sticking to the etching surface and bettering the homogeneity of the deriving porous stratum.

The installation of silicon crystalline after electrochemical etching, as shown by XRD-6000 SHIMADZU Japan, AFM the AFM were taken for porous silicon by AA3000 Scanning Probe Microscope Angstrom Advanced Inc, and FTIR IRAffinity-1 Fourier Transform Infrared Spectrophotometer SHIMADZU and. The AC electrical properties were measured with LCR meter analyzer the frequency between 50 Hz and 5 MHz in the Ministry of Science and Technology.

3. Results and Discussion

3.1 Structural Properties

The skeleton preserve for the constructing of silicon crystalline after electrochemical etching is that it's one important property of porous silicon, studies by X-ray topography. The beam for X-ray is diffracted at appointed angular locations with consideration to the fallen beam relying on the phases of the substate. When crystal magnitude is miniature toward nanometric scale, consequently a width of the peak is immediately reconditioned to the size of the nanocrystalline domains and the expanding of diffraction peaks is spotted [15]. It is well recognized that crystallites size for porous silicon is equals (33.81 nm) can be predestined from diffraction style test by scaling the full width at half maximum (FWHM) measurement and using the Scherrer equation:

$$\boldsymbol{L = k\,\lambda / B\cos\theta_B} \quad \text{..... (1)}$$

Where **K** is the Scherrer constant, **B** is the **FWHM** in radians, λ is the wavelength in nanometers, $\boldsymbol{\theta_B}$ in radians is the diffraction angle and **L** the mean crystallite size [16].

XRD pattern, Figure (1) for etched sample shows diffraction style of PS substance manufactured at anodizing current density of 15 mA/cm^2 at 10 min anodizing times**.** The reflections XRD beam from (100) planes appear two peaks: the first high intensity peak at 2θ = 68.95° from crystal silicon (100) planes, and the second weak intensity peak at 2θ = 69.15°

from PS [17]. The peak in the crystal silicon spectrum is more intense than in the PS spectrum, indicating that the structure crystal silicon contains a crystalline phase [18].

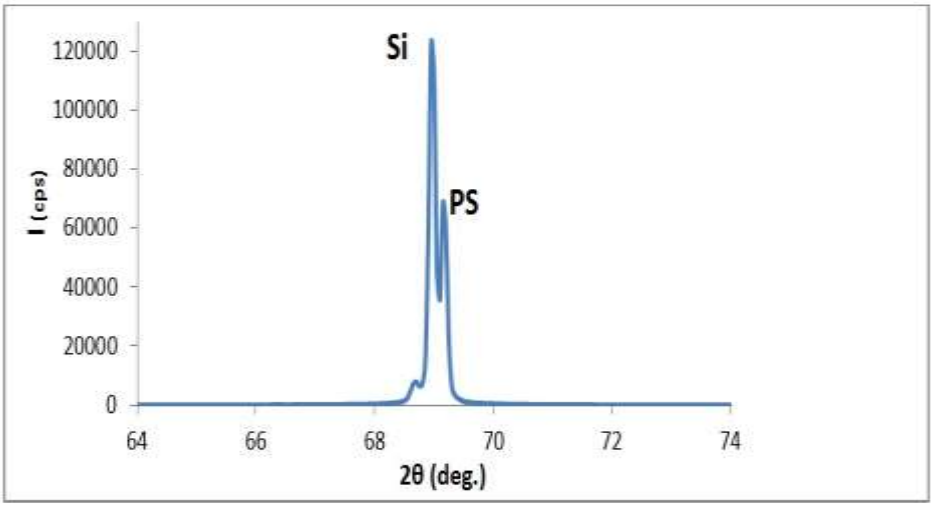

Figure (1) X-ray diffraction of porous silicon primed at anodizing time 10 min and current density 15 mA/cm^2.

3.2 Morphological Characterize

Atomic force microscope (AFM) was using to investigated studies for surface morphology of the oxidized PS layers and focus completely on the nanoscale properties of PS films. The surface morphology of the PS layers primed by anodized etching observations from the AFM graphs could be distinguished. A sponge-like structure was manufactured, show figure (2) displays the morphology of sample primed at etching times of 10 min and the current density was 15 mA/cm^2. The pore sizes produced are with an average diameter of (37.23 nm). When we compare the pore sizes were measured by the reflections XRD beam (33.81 nm) with the pore sizes were measured by the AFM graphs (37.23 nm) the pore sizes were very asymptotic to each other for both measurements.

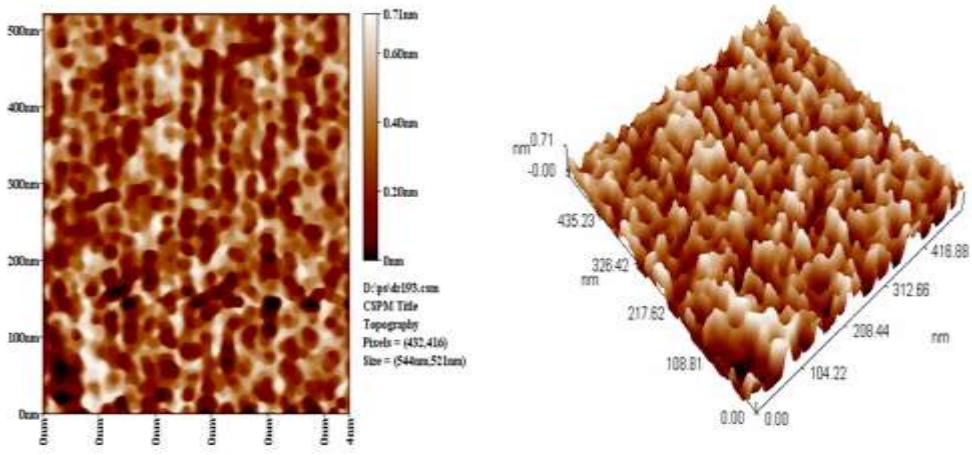

Figure (2) show 2D& 3D AFM images for meso-porous silicon sponge like At 15 mA/cm^2 and etching time 10 min.

3.3 Chemical Structure of PS Layer

Fourier Transform Infrared (FTIR) spectroscopy is best checked for surface chemical structure of PS. Much larger specific area in PS easier to measure than in bulk Si and the FTIR signal in PS is larger. The pore surface includes a high density of dangling bonds of Si for original defect such as hydrogen and fluorine, which are remnants from the electrolyte. If the fabricated PS layer is stockpiled in ambient air for a few hours, the surface oxidizes spontaneously.

The figure (3) shows the FTIR spectrum of the p-type porous silicon. The FTIR spectra tested from sample of: at current density 15 mA/cm^2 and etching time 10 min. The transmittance peak at 623 cm^{-1} Si-H bending in (Si_3-SiH), and 908 cm^{-1} Si-H_2 scissor mode [19, 20]. The transmittance peak at 1107 cm $^{-1}$ are from Si-O-Si stretching modes [21]. Furthermore, 2088cm^{-1} and 2113 cm^{-1} are, respectively, related to Si–H stretch (Si_3-SiH) and Si-H stretch (Si_2-SiH) [22, 19]. The table (3.1) show their IR resonance positions revealed and chemical bonds in PS.

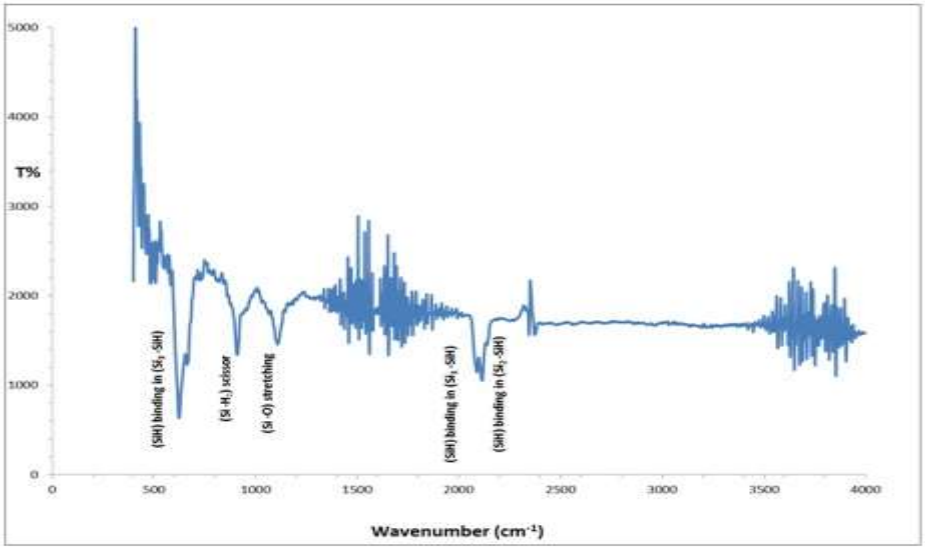

Figure (3) Fourier transform infrared transmittance spectrum of a PS layer 15 mA/cm^2 at etching time 10 min.

Table (1): proportion of the transmittance peaks and wavenumber positions spotted in PS sample by FTIR measurements.

Peak position (cm^{-1})	proportion
623	Si-H bending in (Si_3-SiH)
908	Si-H_2 scissor
1107	Si–O–Si stretching
2088	Si–H stretch (Si_3-SiH)
2113	Si–H stretch (Si_2-SiH)

3.4 Capacitance – Frequency Characteristics

The AC electrical properties were measured with LCR meter analyzer the frequency between 50 Hz and 5 MHz and the 500 mV was measured at room temperature. Figures (4) and (5) show the experiential capacitance as functions of frequency for the bulk silicon and porous silicon etching time was 10 min, and the current density was 15mA/cm^2. The capacitance was found that at low frequency correspond to the barrier

capacitance in the diffusion region (dispersion) at low bias for the substrate studied. Where the barrier capacitance was the capacitance that exists between the p-type and n- type semiconductor materials in a semiconductor pn junction. The capacitance is close to the geometry capacitance in the relaxation region at high frequency [23].

The capacitance values decrease for the sample with porous silicon etching time was 10 min, and the current density was 15mA/cm^2 or lower resistivity. This behavior is attributed to the increasing in the depletion region width which leads to the increasing of built-in potential. However, capacitance decreases with increases the frequency. This indicates clearly the capacitive nature of porous silicon at high frequencies. The reason behaved decreasing of capacitance with high frequencies because the capacitance variation with frequency, since the penetration depth changes with frequency, thus changing the surface-to-depth ratio of the material involved in the electromagnetic interaction and the shape of curve for porous silicon like the zigzag because the PSi material used in this paper shows an anisotropic morphology, capacitance is also anisotropic.

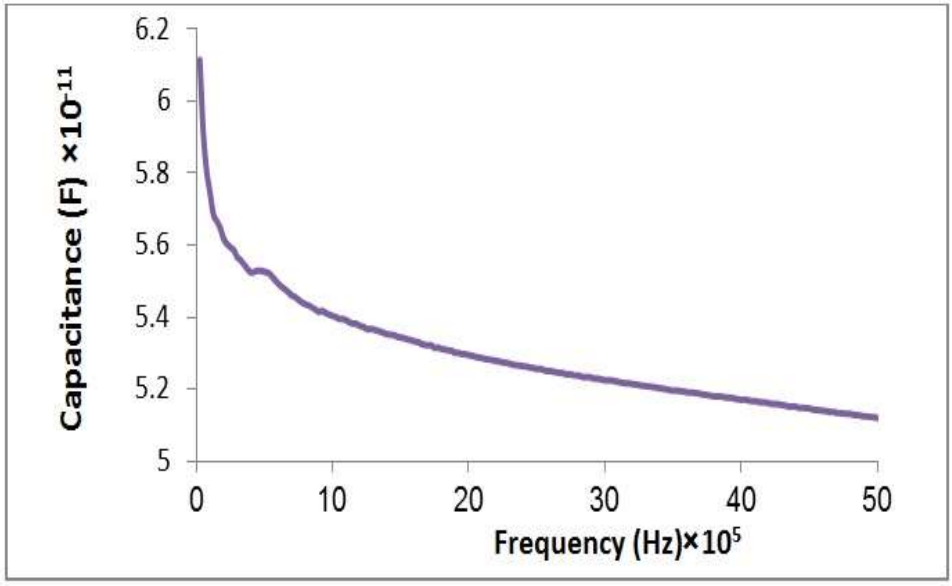

Figure (4) the capacitance as functions of frequency for the bulk silicon

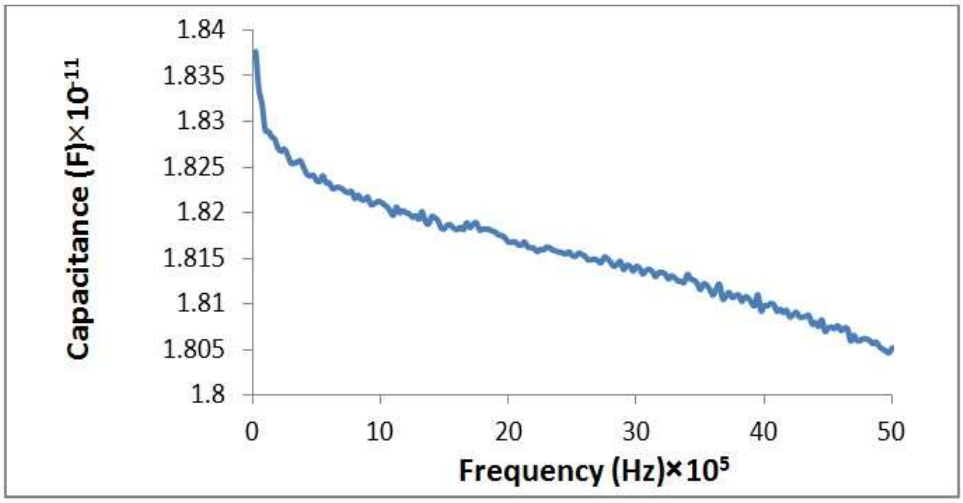

Figure (5) the capacitance as a functions of frequency for the porous silicon etching time was 10 min, and the current density was 15mA/cm^2

3.5 Dielectric – Frequency Characteristics

Microscopic models for determining porous silicon dielectric properties. Porous silicon composition and morphology used for its formation as well as on the starting wafer resistivity depend on the electrochemical conditions. Its dielectric properties are highly dependent on its structure and morphology. several works were worked in the literature that correlate the material structure with its dielectric properties. According to [24, 25, 26], the ac electrical transport of porous silicon follows mechanism.

In the very low frequency range the length of the carrier random walk during the fractal build of the material is valid, while at higher frequencies, the random path is shorter and the hopping length stops to be the critical factor. In that case, conduction is mainly specific by the distance between inhomogeneous areas [26]. The dielectric permittivity of porous silicon describes the defect inside the material and the polarization of the atoms. The dielectric permittivity for bulk silicon higher than porous silicon that occurs at low frequencies that attributed to the density variation between the bulk and porous silicon. the presence of porous which give the structure less density for porous silicon and the dielectric permittivity for both bulk and porous silicon decreases with increases the frequency as shown in figures (6) and (7).

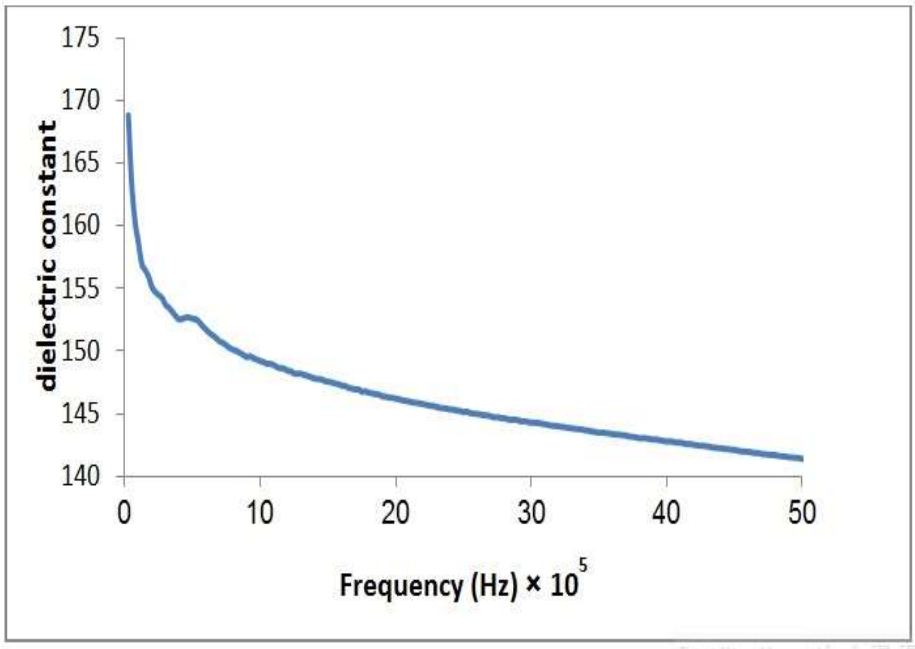

Figure (6) Dielectric permittivity of bulk silicon as a function of frequency.

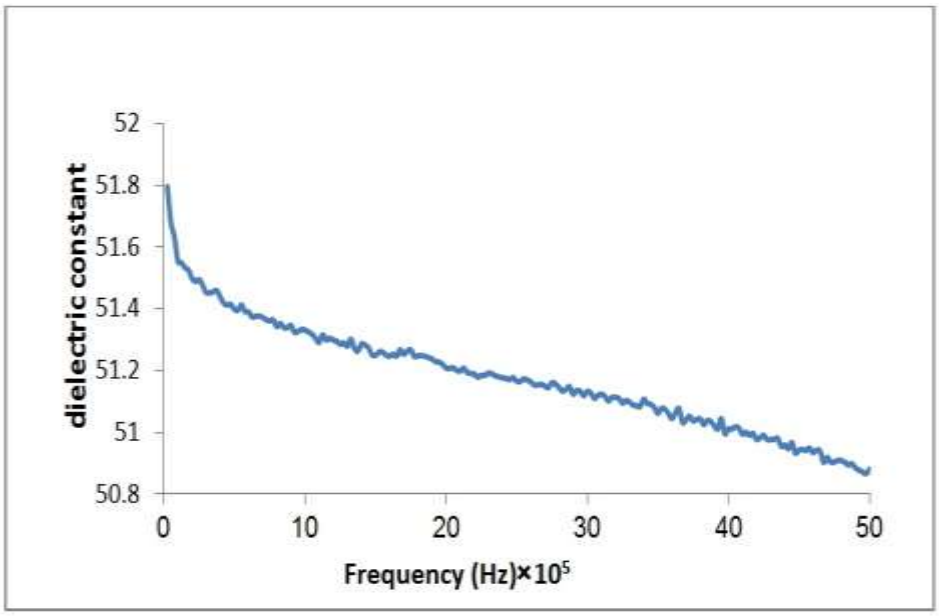

Figure (7) Dielectric permittivity as a function of frequency for the porous silicon etching time was 10 min, and the current density was 15mA/cm^2

3.6 Loss tangent (tan δ_D) - Frequency Characteristics

The loss tangent most ceramics rise almost linearly as frequency increases; in this cases, it is likely to extrapolate measurement data from one frequency range to another. Materials of very low-loss possess loss tangents in the microwave spectrum that are nearly frequency independent. In materials with a finite dc conductivity imaginary portion of the permittivity increases at low frequencies as $1/\omega$ where ω is radial frequency, (for example, < 1 kHz). Conducting materials are difficult to measure at low frequencies (f < 1 MHz). This is because the boundary layer between the substance and electrode produces an electrode-polarization capacitance that must be neglected from the measurement result.

Figures (8) and (9) loss tangent (tan δ_D) versus of frequency for bulk silicon and porous silicon respectively show the loss tangent (tan δ_D) for bulk silicon higher than porous silicon etching time was 10 min, and the current density was 15mA/cm^2 at low frequencies for 3 MHz and the bulk silicon equal almost with porous silicon for loss tangent versus frequency from 3MHz to 5MHz .

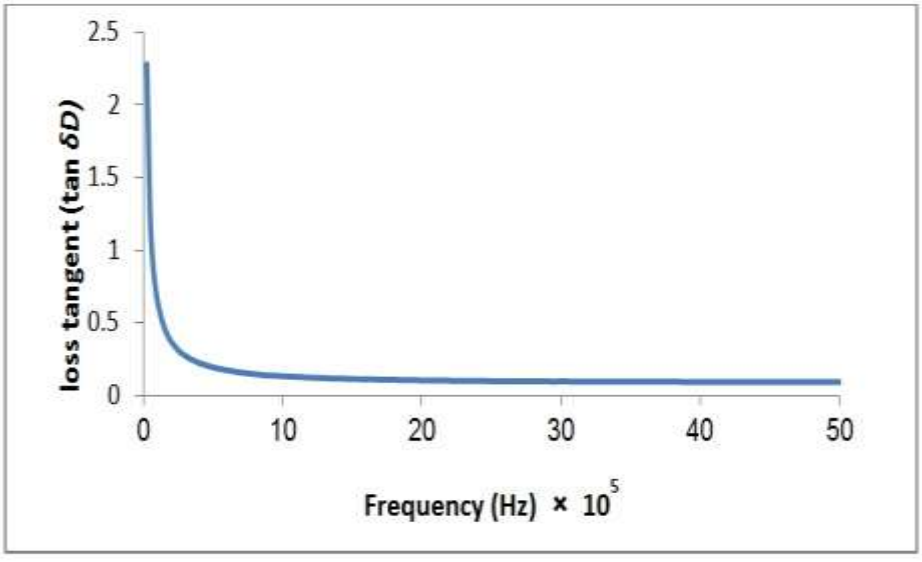

Figure (8) loss tangent (tan δ_D) of bulk silicon versus of frequency.

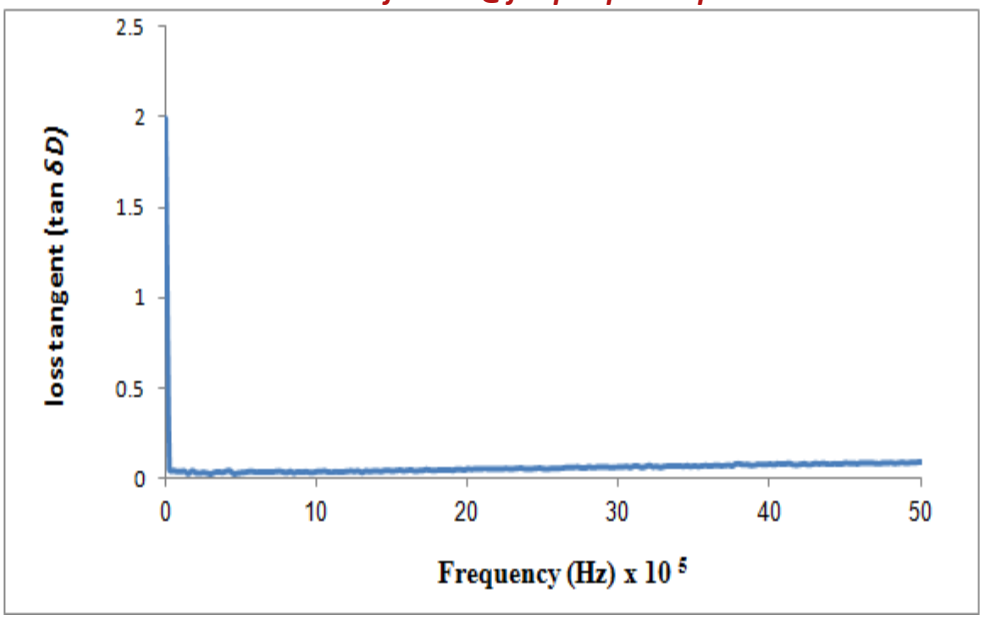

Figure (9) loss tangent (tan δ_D) versus of frequency for the porous silicon etching time was 10 min, and the current density was 15mA/cm^2.

CONCLUSIONS

The silicon grain size and the porous structure were decreased that it was observed from a broadenning of the silicon peaks from the XRD properties. The oxygen is normally missing, the dominant bonds being Si-H groups in porous silicon.

The AFM realization display the rough silicon surface which can be uniformed as a condensation point for small a sponge-like structure which plays an paramount role for the propertied the nanocrystalline porous silicon. The capacitance values decrease for the sample with porous silicon and this behavior is imputed to the rising in the depletion region width which leads to the increasing of built-in potential. However, capacitance decreases with increases the frequency. The dielectric permittivity for bulk silicon more than porous silicon at low frequencies and the dielectric permittivity for both bulk and porous silicon decreases with increases the frequency. The loss tangent (tan δ_D) for bulk silicon higher than porous silicon at low frequencies for 3 MHz and the bulk silicon equal almost

with porous silicon for loss tangent versus frequency from 3MHz to 5MHz.

References

[1] Andrea Edit Pap. Investigation of Pristine and Oxidized Porous Silicon // Faculty of technology, University of Oulu, Finland, 2005, P. 13–45.

[2] V.A. Skryshevsky, Photoluminescence of inhomogeneous porous silicon at gas adsorption, Appl. Surf. Sci. 157 (2000) 145–150.

[3] by Josefine Helene Selj : Porous Silicon for Light Management in Silicon Solar Cells: Thesis submitted for the degree of Philosophiae Doctor Department of Physics University of Oslo December 2010

[4] Jung-Keun Yoo1 , Jongsoon Kim2 , Hojun Lee1 , Jaesuk Choi1 , Min-Jae Choi1 , Dong Min Sim2 , Yeon Sik Jung1,3 and Kisuk Kang2,3 :Porous silicon nanowires for lithium rechargeable batteries: Nanotechnology 24 (2013) 424008 (7pp).

[5] A. Porcher, B. Remaki, C. Populaire, and D. Barbier, "Nanostructured porous silicon as thick electrical insulator for radio-frequency applications,"Phys. Stat. Sol. A, vol. 204, no. 6, pp. 1653–1657, Jun. 2007.

[6] Van Hoi Pham, Thuy Van Nguyen, The Anh Nguyen, Van Dai Pham and Huy Bui Nano porous silicon microcavity sensor for determination organic solvents and pesticide in water . Advances in Natural Sciences: Nanoscience and Nanotechnology 5 (2014) 045003 (9pp).

[7] Georgiy V Tkachenko, Volodymyr Tkachenko, Luca De Stefano and Igor A Sukhoivanov Tunable NIR filter based on a free-standing porous silicon film containing nematic liquid crystal Journal of Optics A: Pure and Applied Optics 2009 Volume 11, Number 10.

[8] Guoguang Rong1, Jarkko J. Saarinen2, John E. Sipe2, and Sharon M. Weiss1 :High Sensitivity Sensor Based on Porous Silicon Waveguide : Materials Research Society 2006 , Vol. 934

[9] by Josefine Helene Selj : Porous Silicon for Light Management in Silicon Solar Cells: Thesis submitted for the degree of Philosophiae Doctor Department of Physics University of Oslo December 2010

[10] Kabbi, H., Miliki, N., Cheynet, M., Saikalay, W., Gibbert, D., Bassïs, B., Yangui, B. and Charï, A. (2006) Structural and Optical Properties of Vapour-Etching Based Porous Silicon. Crystal Research and Technology, 41, 154-162.

[11] L. Remache1, A. Mahdjoub2, E. Fourmond1, J. Dupuis1, M. Lemiti1 : Design of porous silicon /PECVD SiOx antireflection coatings for silicon solar cells International Conference on Renewable Energies and Power Quality Granada (Spain), 2010, Vol.1, No.8,

[12] M. Al-Amin1 and A. Assi*2 : Efficiency improvement of crystalline silicon solar cells : Materials and processes for energy communicating current research and technological development 2013

[13] L. Remache, A. Mahdjoub, E. Fourmond, J. Dupuis, M. Lemiti, "Design of porous silicon /PECVD SiOx antireflection coatings for silicon solar cells" International Conference on Renewable Energies and Power Quality vol. 192, 596-598 (2010).

[14] W. J. Salcedo, F. J. R. Fernandez, E. Galeazzo, " St ruct ural Characterization of Photoluminescent Porous Silicon with FTIR Spect roscopy", Brazilian Journal of Physics, Vol. 27, No. 4, 158- 161(1997).

[15] Lorusso, A. V. Nassisi, G. Congedo, N. Lovergine, L. Velardi, P. Prete, "Pulsed plasma ion source to create Si nanocrystals in SiO2 substrates", Applied Surface Science, 255, 5401-5404 (2009).

[16] Luigi Russo, Francesco Colangelo, Raffaele Cioffi, Ilaria Rea and Luca De Stefano, "A Mechanochemical Approach to Porous Silicon Nanoparticles Fabrication", Materials 4, 1023-1033 (2011).

[17] Qadeer Hussain, Arifullah, Nazir A. Naz, Ammar Akbar, Akbar Ali " Structural Characteristics of Porous Silicon " Journal of Surface Engineered Materials and Advanced Technology, 2014, 4, 105-110

[18] Sonia Ben Slama ,Messaoud Hajji ,Hatem Ezzaouia, " Crystallization of amorphous silicon thin films deposited by PECVD on nickel-metalized porous silicon" Nanoscale Research Letters, 7 , 464 (2012).

[19] Bisis, S. Ossicini and L. Pavesi, "porous silicon: a quantum sponge structure for silicon based optoelectronics", Surface science reports 264, (2000).

[20] Arce, R.D. R.R. Koropecki, G. Olmos, A.M. Gennaro, J.A. Schmidt, "Photoinduced Phenomena in Nanostructured Porous Silicon", Thin Solid Films 510, 169-174 (2006).

[21] Yue Zhao, Deren Yang, Dongsheng Li, Minghua Jiang, "Annealing and amorphous silicon passivation of porous silicon with blue light emission", Applied Surface Science 252, 1065–1069 (2005).

[22] PAP, A. E. "Investigation of Pristine and Oxidized Porous Silicon", Thesis University of Oulu, (2005).

[23] F. Fonthal, C. Goyes, A. Rodríguez " Electrical Transport and Impedance Analysis of Au/Porous Silicon Thin Films " Electronics, Robotics and Automotive Mechanics Conference 2008, 25 No. 115 - 85,

[24]. Lehmann V, Hofmann F, Möller F, Grüning U: Resistivity of porous silicon: a surface effect. Thin Solid Films 1995, 255:20–22.

[25]. Ben-Chorin M, Möller F, Koch F: Nonlinear electrical transport in porous silicon. Phys Rev B 1994, 49:2981–2984.

[26]. Ben-Chorin M, Möller F, Koch F, Schirmacher W, Eberhard M: Hopping transport on a fractal: ac conductivity of porous silicon. Phys Rev B 1995, 51:2199–2213.